

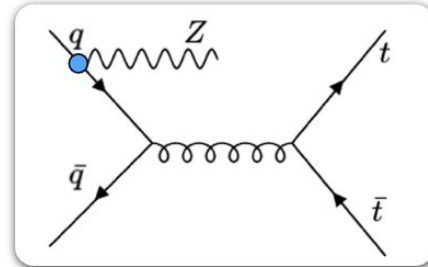
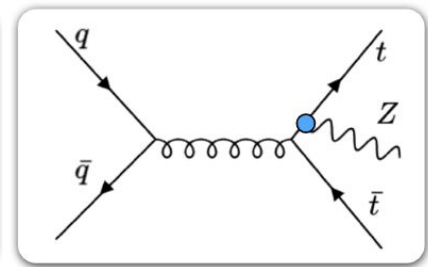
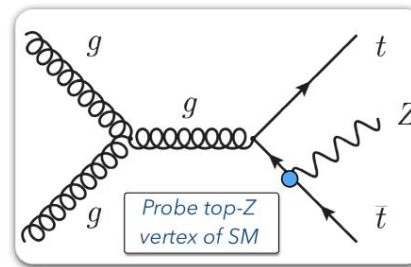
Inclusive and differential $t\bar{t}Z$ cross-section measurement, including interpretations, with the full ATLAS Run 2 dataset

**Dominik Babál (Slovak Academy of Sciences)
on behalf of the ATLAS Collaboration**

LHC TOP WG meeting (29.11.2023)

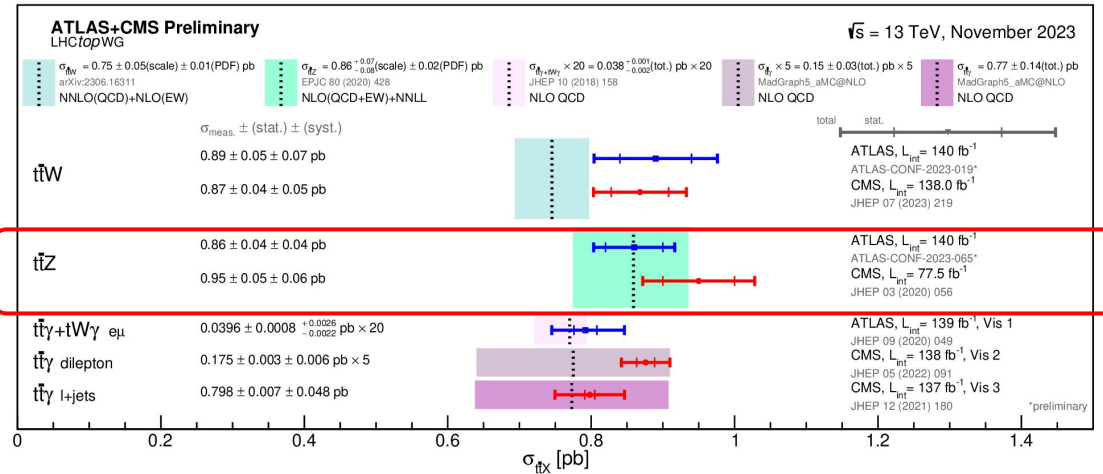
Introduction

- $t\bar{t}Z$ - rare process → provides stringent tests of SM
- Important background for LHC searches ($t\bar{t}H$, $t\bar{t}t\bar{t}$, tZ , BSM searches)
- Sensitivity to **BSM physics** affecting **tZ coupling**
- Measurements aimed at improving previous inclusive and differential results + adding SMEFT and spin-correlations interpretation



[ATLAS-CONF-2023-065](#)

- Refined measurement **building upon previous ATLAS result** ([EPJC 81 \(2021\) 737](#))
- $Z \rightarrow e\bar{e}/\mu\bar{\mu}$, 3 channels according to $t\bar{t}$ decay → **2I** - all hadronic, **3I** - l+jets, **4I** - dileptonic)



Analysis overview

This analysis:

- Full Run 2 data (140 fb⁻¹)
- Legacy ttZ measurement
- Improving previous result **using same dataset**



Previous ttZ results:

inclusive + differential 13 TeV; 139 fb⁻¹
[EPJC 81 \(2021\) 737](#)

$$\sigma_{t\bar{t}Z} = 0.99 \pm 0.05(\text{stat.}) \pm 0.08(\text{syst.}) \text{ pb}$$

$$\frac{\delta\sigma_{t\bar{t}Z}}{\sigma_{t\bar{t}Z}} \approx 9.5\%$$



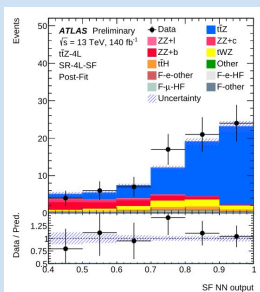
inclusive + differential + EFT 13 TeV; 77.5 fb⁻¹
[JHEP 03 \(2020\) 056](#)

$$\sigma_{t\bar{t}Z} = 0.95 \pm 0.05(\text{stat.}) \pm 0.06(\text{syst.}) \text{ pb}$$

$$\frac{\delta\sigma_{t\bar{t}Z}}{\sigma_{t\bar{t}Z}} \approx 8.2\%$$

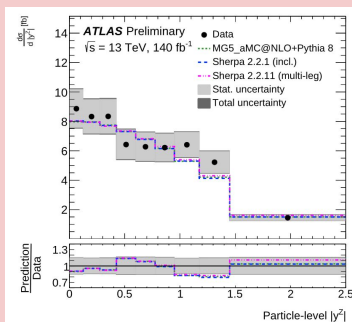
1.) Inclusive xs

- Addition of **2IOS channel** (previously only 3I and 4I)
- **DNNs** for region definitions and fit input



2.) Differential xs

- **New variables** (17 vs. 9)
- New unfolding technique (PLU) with regularisation



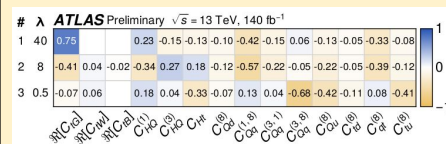
3.) Spin correlations

- **First interpretation** for ttZ
- **9 angular distributions**
- **Detector-level fit**

Distribution	Channel	Expected values	Observed values
$\cos \varphi$	3l + 4l	+1.39 -1.38	-0.09 ^{+1.34} -1.28
$\cos \theta_r^+$ · cos θ_r^-	3l + 4l	+1.83 -1.82	1.17 ^{+1.80} -1.76
$\cos \theta_n^+$ · cos θ_n^-	3l + 4l	+1.78 -1.78	1.39 ^{+1.72} -1.73
$\cos \theta_n^+$ · cos θ_r^-	3l + 4l	+1.87 -1.86	-1.05 ^{+2.06} -1.96
$\cos \theta_r^+$ · cos θ_n^- + cos θ_r^- · cos θ_n^+	3l + 4l	+1.93 -1.93	0.36 ^{+1.99} -1.93
$\cos \theta_r^+$	3l + 4l	+1.81 -1.80	1.56 ^{+1.86} -1.98
$\cos \theta_r^-$	3l + 4l	+1.82 -1.78	1.81 ^{+1.63} -1.68
$\cos \theta_n^+$	3l + 4l	+1.69 -1.67	2.00 ^{+1.65} -1.70
$\cos \theta_n^-$	3l + 4l	+1.68 -1.68	2.31 ^{+1.68} -1.68

4.) EFT interpretation

- **20 dim-6 operators**
- Linear and quadratic fits
- **Fisher information matrix**



Analysis regions

Dilepton

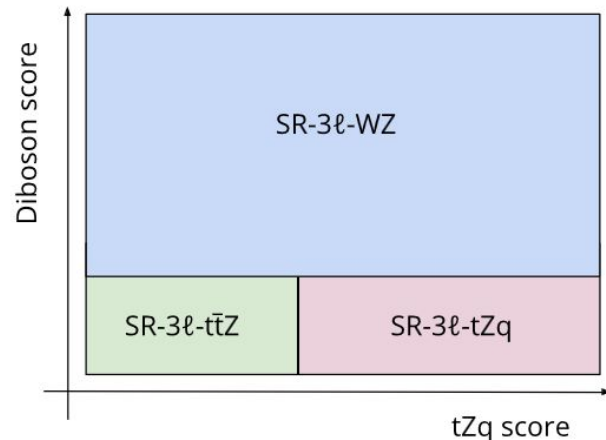
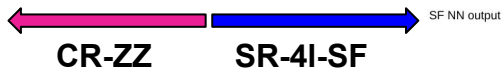
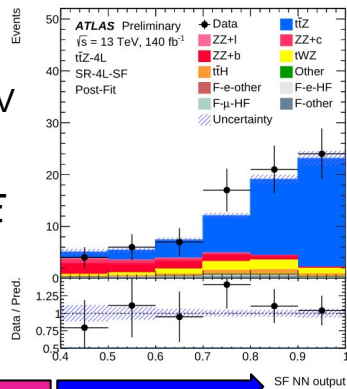
- **1 OSSF (opposite-sign-same-flavour) lepton pair** with $|m_{ll}-m_Z| < 10$ GeV
- $p_T^l > 30, 15$ GeV
- SRs inspired by the **36 fb⁻¹ analysis**
- **3 SRs based on jet and b-jet multiplicity:**
 - **SR-2l-5j2b, SR-2l-6j1b, SR-2l-6j2b**

Trilepton

- At least **1 OSSF lepton pair** with $|m_{ll}-m_Z| < 10$ GeV
- $p_T^l > 27, 20, 15$ GeV
- At least 3 jets and **1 b-tagged jet (@85% WP)**
- **3 orthogonal SRs** based on output nodes from **multi-class DNN**:
 - **SR-3l-ttZ, SR-3l-tZq, SR-3l-WZ**

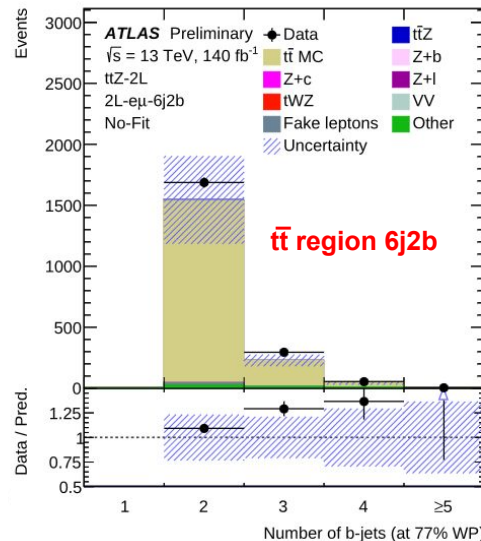
Tetralepton

- At least **1 OSSF lepton pair** with $|m_{ll}-m_Z| < 20$ GeV
- $p_T^l > 27, 7, 7, 7$ GeV
- At least 2 jets and **1 b-tagged jet (@85% WP)**
- **2 SRs based on flavor of the lepton pair from tt**
 - **SR-4l-SF, SR-4l-DF**
- **DNN > 0.4 used to define SF region** - remaining part used for ZZ control region



2l channel strategy

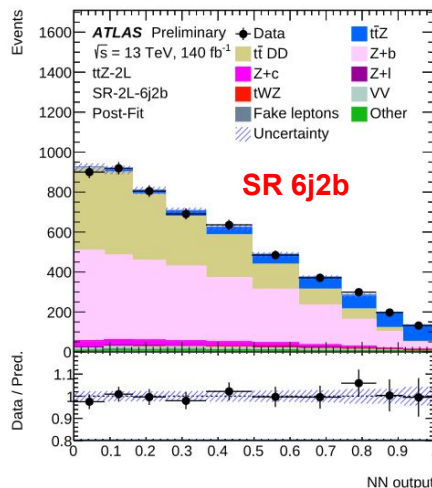
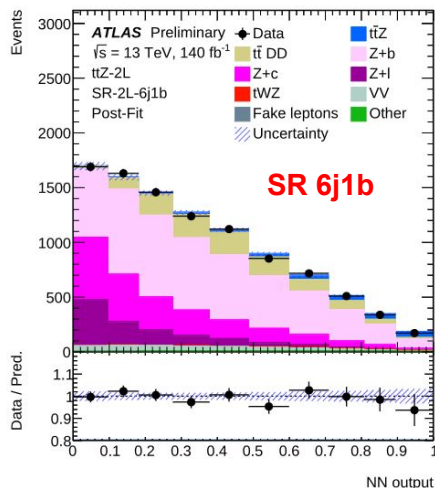
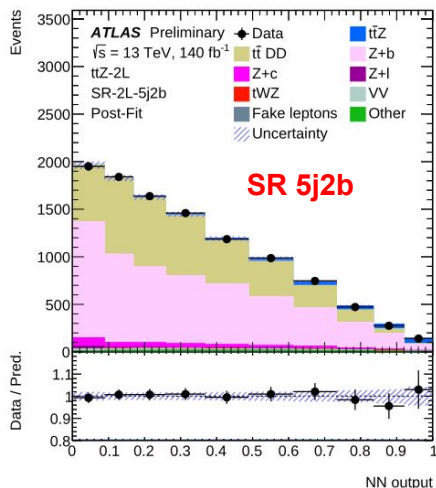
- 2l channel **only** in the **inclusive** measurement
- **DNN** outputs in each SR used for **Profile likelihood fit (PLF)**
- Dominant backgrounds: **dileptonic $t\bar{t}$** and **Z+jets**
- **Normalisations** of **Z+b** and **Z+c** free parameters of the fit



$t\bar{t}$ poorly modelled \rightarrow data-driven estimate:

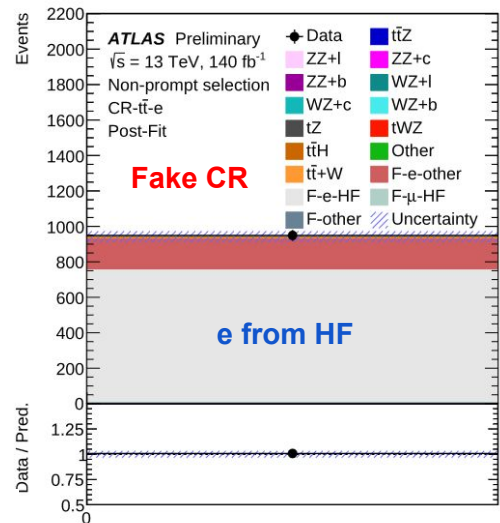
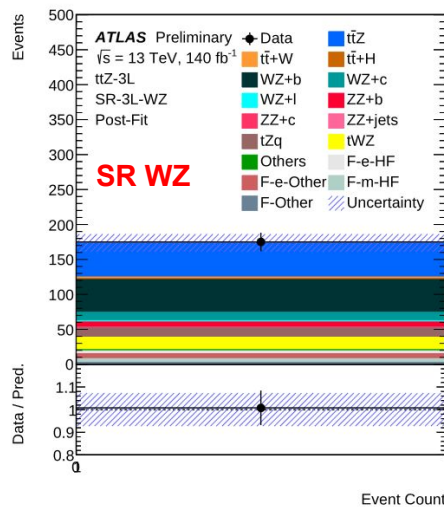
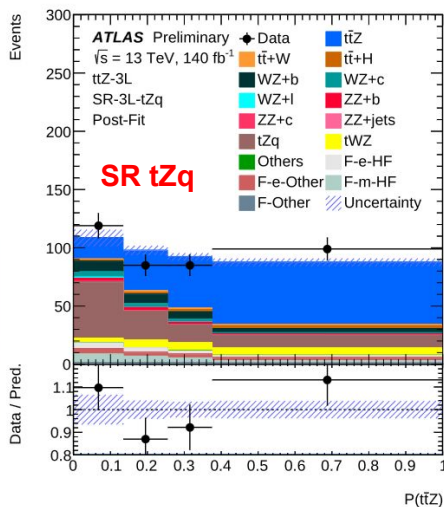
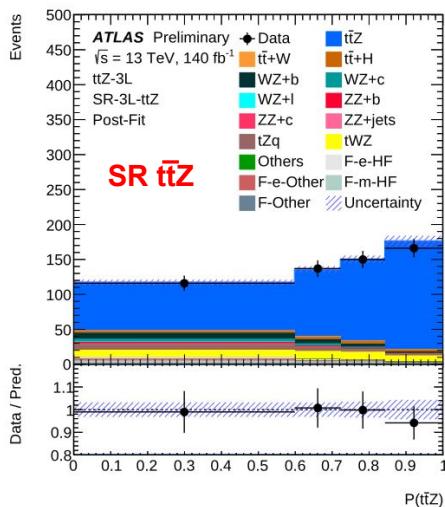
- $t\bar{t}$ regions defined similar to SRs, but OSSF \rightarrow OSDF
- Very pure regions
- $t\bar{t}$ estimation in SRs = (data in $t\bar{t}$ regions - non- $t\bar{t}$ background in $t\bar{t}$ regions) $\cdot C_{t\bar{t}}$

$$C_{t\bar{t}} = \frac{N_{t\bar{t}}^{\ell\ell}}{N_{t\bar{t}}^{e\mu}}$$



3l channel strategy

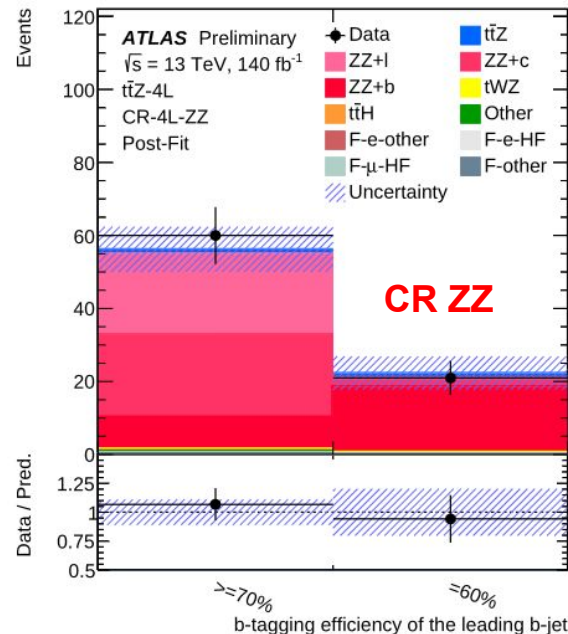
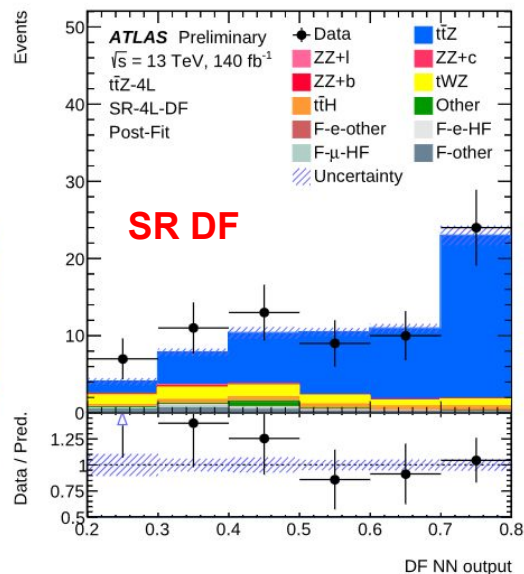
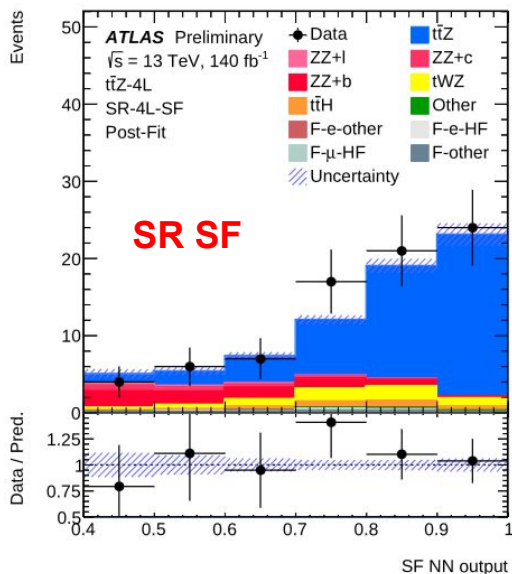
- Multi-class DNN - $\bar{t}\bar{t}Z$, tZq , WZ output nodes
- $\bar{t}\bar{t}Z$ node output fitted, tZq and WZ used for SR definitions
- $WZ+b$ normalisation measured in the fit
- tZq fixed to SM (low stats)



- Non-prompt/fake leptons relevant for 3l and 4l - dedicated CRs
- 4 categories defined using loose selection
 - F-e-HF
 - F- μ -HF
 - F-e-Other
 - F-Other (form MC)

4l channel strategy

- Leading backgrounds: **tWZ** and **ZZ+jets**
- **DNN outputs** used as an input for the fit
- Irreducible **tWZ** - estimated from **MC** (low stats)



- **ZZ+jets** mostly in **SF** region
- **ZZ CR** for SF selection - defined with $\text{DNN} < 0.4$
- **ZZ+b** normalisation **extracted in the fit** \rightarrow **CR** with **two bins based on b-tagging efficiency**

Inclusive $\tau\tau$ measurement

- Simultaneous **profile likelihood fit** in all SRs and CRs
- **12 regions** (8 SRs and 4 CRs) and **8 free parameters** in the combined fit
- Extracted **signal strength ($\mu_{\tau\tau Z}$) translated to the cross section** and corrected to match fiducial region ($70 < m_{\tau\tau} < 110$ GeV)
- **Main improvements:** DNNs, better modelling, region definitions, addition of 2l channel
- **35% reduction in uncertainty when compared to previous $\tau\tau Z$**

Channel	$\sigma_{\tau\tau Z}$
Dilepton	0.84 ± 0.11 pb = 0.84 ± 0.06 (stat.) ± 0.09 (syst.) pb
Trilepton	0.84 ± 0.07 pb = 0.84 ± 0.05 (stat.) ± 0.05 (syst.) pb
Tetralepton	$0.97^{+0.13}_{-0.12}$ pb = 0.97 ± 0.11 (stat.) ± 0.05 (syst.) pb
Combination (2l, 3l & 4l)	0.86 ± 0.06 pb = 0.86 ± 0.04 (stat.) ± 0.04 (syst.) pb

Uncertainty Category	$\Delta\sigma_{\tau\tau Z}/\sigma_{\tau\tau Z}$ [%]
Background normalisations	2.0
Jets and E_T^{miss}	1.9
b -tagging	1.7
$\tau\tau Z$ μ_F and μ_R scales	1.6
Leptons	1.6
Z +jets modelling	1.5
tWZ modelling	1.1
$\tau\tau Z$ showering	1.0
$\tau\tau Z$ A14	1.0
Luminosity	1.0
Diboson modelling	0.8
tZq modelling	0.7
PDF (signal & backgrounds)	0.6
MC statistical	0.5
Other backgrounds	0.5
Fake leptons	0.4
Pile-up	0.3
Data-driven $\tau\tau$	0.1

Previous $\tau\tau Z$

2.9

2.3

2.9

3.1

sub-leading
leading

2.8

2.6

EPJC 79 (2019) 249

$$\sigma_{\tau\tau Z}^{\text{NLO}} = 0.86 \pm 0.08(\text{scale}) \pm 0.03(\text{PDF}) \text{ pb}$$

$$\frac{\delta\sigma_{\tau\tau Z}}{\sigma_{\tau\tau Z}} \approx 6.5\%$$

$$\frac{\delta\sigma_{\tau\tau Z}^{\text{NLO}}}{\sigma_{\tau\tau Z}^{\text{NLO}}} \approx 10\%$$

Differential measurements

- Only in 3l and 4l channels
- Profile likelihood unfolding (PLU) to particle and parton level
- PLU allows for:
 - inclusion of **multiple SRs and CRs**,
 - free floating normalisation of the leading backgrounds,
 - **pulls and constraints** of the uncertainties
- Absolute and normalised distributions
- 17 observables (**5 in 3l**, **3 in 4l** and **9 in combination**)
- **Tikhonov regularisation** for observables featuring hadronic top

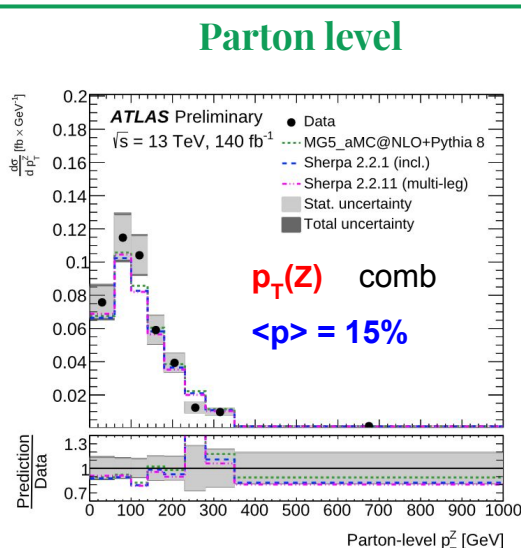
$$R(\vec{\mu}) = \exp \left[-\frac{\tau^2}{2} \sum_{i=2}^{i+1 < N_{bins}} ((\mu_i - \mu_{i-1}) - (\mu_{i+1} - \mu_i))^2 \right],$$

	Variable	Regularisation	τ^{particle}	τ^{parton}
3 ℓ + 4 ℓ	p_{T}^Z	No	-	-
	$ y^Z $	No	-	-
	$\cos \theta_Z^*$	No	-	-
	p_{T}^l	Yes	1.5	1.4
	$p_{\text{T}}^{t\bar{t}}$	Yes	1.6	1.5
	$ \Delta\phi(t\bar{t}, Z) $	Yes	2.4	2.1
	$m^{t\bar{t}Z}$	Yes	1.5	1.6
	$m^{t\bar{t}}$	Yes	1.5	1.4
	$ y^{t\bar{t}Z} $	Yes	1.5	1.5
3 ℓ	H_{T}^{ℓ}	No	-	-
	$ \Delta\phi(Z, t_{\text{lep}}) $	No	-	-
	$ \Delta y(Z, t_{\text{lep}}) $	No	-	-
	$p_{\text{T}}^{\ell, \text{non-Z}}$	No	-	-
	N_{jets}	No	-	-
4 ℓ	H_{T}^{ℓ}	No	-	-
	$ \Delta\phi(\ell_t^+, \ell_{\bar{t}}^-) $	No	-	-
	N_{jets}	No	-	-

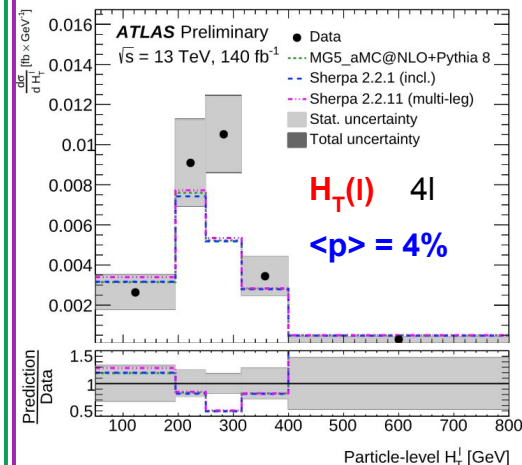
Differential results

- Unfolded distributions compared to:
 - MG5_aMC@NLO + Pythia 8 (nominal)
 - Sherpa 2.2.1 (inclusive)
 - Sherpa 2.2.11 (multi-leg)
- In general **good agreement** - some observables **suffer from bad modelling** → lower p-values for $H_T(l)$, $|\Delta y(Z, t^{\bar{t}})|$, $p_T^{t\bar{t}}$
- Particle level more precise** (more diagonal migration matrices)
- Measurement **statistically limited** (but **30% improvement** when compared to previous $t\bar{t}Z$ analysis thanks to PLU, DNN, ...)

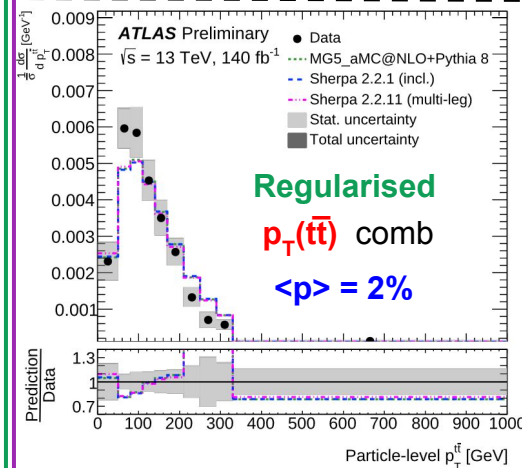
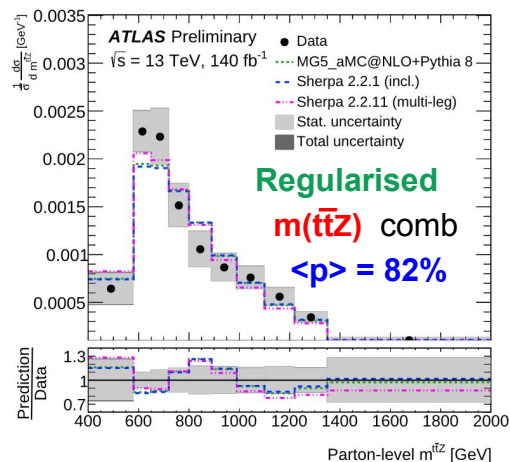
Absolute



Particle level



Normalised



Spin correlations interpretation

- **First evidence** of top-quark spin correlations in $t\bar{t}Z$ (SM expectations modified by the Z boson)
- 6 independent observables (in $t\bar{t}$ rest frame):

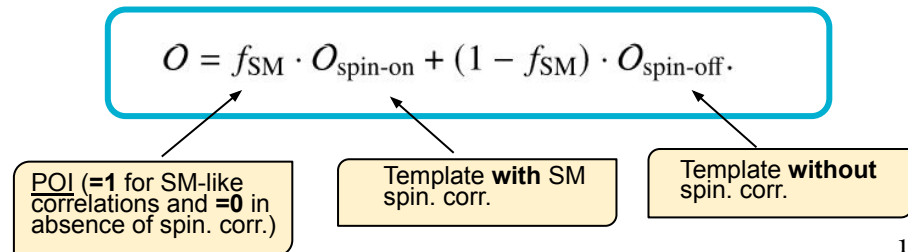
$\cos \theta_k^+, \cos \theta_k^-, \cos \theta_n^+, \cos \theta_n^-, \cos \theta_r^+, \cos \theta_r^-$
- Observables defined using **leptons from $t\bar{t}$** (or **lepton + down-type quark** from W decay)

Coefficient	Expression	
c_{rr}	$-9\langle \cos \theta_r^+ \cdot \cos \theta_r^- \rangle$	spin corr.
c_{kk}	$-9\langle \cos \theta_k^+ \cdot \cos \theta_k^- \rangle$	
c_{nn}	$-9\langle \cos \theta_n^+ \cdot \cos \theta_n^- \rangle$	
c_{rk}	$-9\langle \cos \theta_r^+ \cdot \cos \theta_k^- + \cos \theta_r^- \cdot \cos \theta_k^+ \rangle$	spin cross corr.
c_{kn}	$-9\langle \cos \theta_k^+ \cdot \cos \theta_n^- + \cos \theta_k^- \cdot \cos \theta_n^+ \rangle$	
c_{rn}	$-9\langle \cos \theta_r^+ \cdot \cos \theta_n^- + \cos \theta_r^- \cdot \cos \theta_n^+ \rangle$	
c_r	$-9\langle \cos \theta_k^+ \cdot \cos \theta_n^- - \cos \theta_k^- \cdot \cos \theta_n^+ \rangle$	
c_k	$-9\langle \cos \theta_n^+ \cdot \cos \theta_r^- - \cos \theta_n^- \cdot \cos \theta_r^+ \rangle$	
c_n	$-9\langle \cos \theta_r^+ \cdot \cos \theta_k^- - \cos \theta_r^- \cdot \cos \theta_k^+ \rangle$	
b_r^+	$3\langle \cos \theta_r^+ \rangle$	polarisations
b_r^-	$3\langle \cos \theta_r^- \rangle$	
b_k^+	$3\langle \cos \theta_k^+ \rangle$	
b_k^-	$3\langle \cos \theta_k^- \rangle$	
b_n^+	$3\langle \cos \theta_n^+ \rangle$	
b_n^-	$3\langle \cos \theta_n^- \rangle$	

Consider only 9 coefficient that are non-0 within theoretical uncertainties

Strategy:

- **Template fit** of detector-level distributions (unfolded distributions unusable -> would require regularisation in 4l)
- Each observable O fitted to **lin. combination of spin-on and spin-off hypotheses**



$$O = f_{\text{SM}} \cdot O_{\text{spin-on}} + (1 - f_{\text{SM}}) \cdot O_{\text{spin-off}}$$

Spin correlations interpretation

- Coefficients fitted **individually** and then **combined** using profiled χ^2 fit (with stat. and syst. correlations)

opening angle between charged leptons (or lepton and s-jet)

Distribution	Channel	Expected values	Observed values
$\cos \varphi$	$3\ell + 4\ell$	$1^{+1.39}_{-1.38}$	$-0.09^{+1.34}_{-1.28}$
$\cos \theta_r^+ \cdot \cos \theta_r^-$	$3\ell + 4\ell$	$1^{+1.83}_{-1.82}$	$1.17^{+1.80}_{-1.76}$
$\cos \theta_k^+ \cdot \cos \theta_k^-$	$3\ell + 4\ell$	$1^{+1.78}_{-1.78}$	$1.39^{+1.72}_{-1.73}$
$\cos \theta_n^+ \cdot \cos \theta_n^-$	$3\ell + 4\ell$	$1^{+1.87}_{-1.86}$	$-1.05^{+2.06}_{-1.96}$
$\cos \theta_r^+ \cdot \cos \theta_k^- + \cos \theta_r^- \cdot \cos \theta_k^+$	$3\ell + 4\ell$	$1^{+1.93}_{-1.93}$	$0.36^{+1.99}_{-1.93}$
$\cos \theta_r^+$	$3\ell + 4\ell$	$1^{+1.81}_{-1.80}$	$1.56^{+1.86}_{-1.98}$
$\cos \theta_r^-$	$3\ell + 4\ell$	$1^{+1.82}_{-1.78}$	$1.81^{+1.63}_{-1.68}$
$\cos \theta_k^+$	$3\ell + 4\ell$	$1^{+1.69}_{-1.67}$	$2.00^{+1.65}_{-1.70}$
$\cos \theta_k^-$	$3\ell + 4\ell$	$1^{+1.68}_{-1.68}$	$2.31^{+1.68}_{-1.68}$

- Measurement consistent with the SM prediction, but **statistically limited**
- **Spin-off hypothesis rejected with 1.8σ**
- Main systematics from **MC modelling**, E_T^{miss} and **flavour tagging**

$$f_{\text{SM}}^{\text{obs.}} = 1.20 \pm 0.63 \text{ (stat.)} \pm 0.25 \text{ (syst.)} = 1.20 \pm 0.68 \text{ (tot.)}$$

SMEFT interpretation

- $t\bar{t}Z$ sensitive to 20 dim-6 operators (6 top-boson, 14 four-quark)
- Particle level normalised differential distributions taken as an input (reweighted with **LO** parametrisation)
- Separate fits for top-boson and four-quark operators

$$O = O_{\text{SM}} + \sum_i C_i A_i + \sum_{i,j} C_i C_j B_{ij}.$$

- **3 fit strategies:**

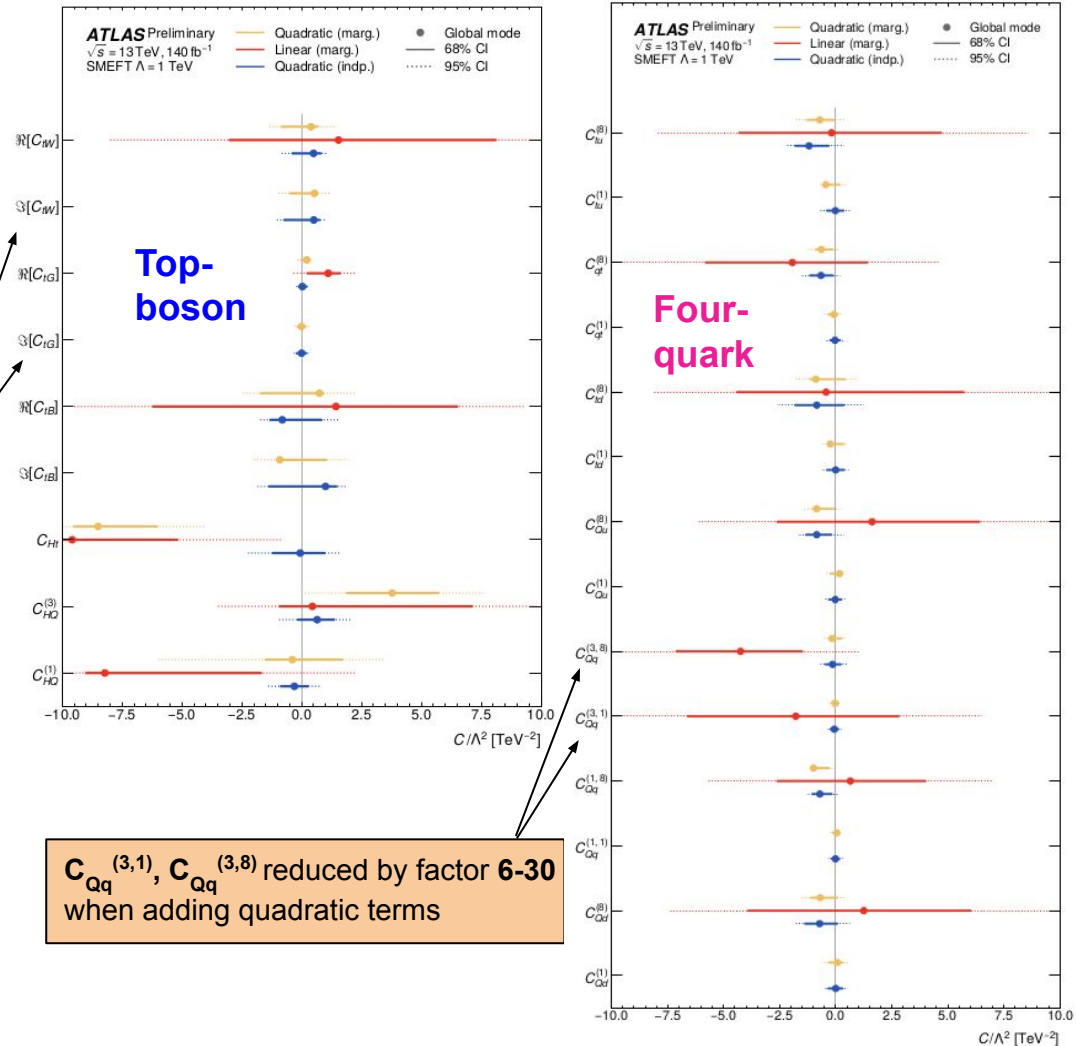
- Simple **linear fit** (linear term A \rightarrow interference between SM and SMEFT)
- Full **quadratic fit** (both linear A and quadratic B terms)
- Individual **quadratic fit** (all other operators set to 0, for comparison with other analyses)

Observables used:

- p_T^Z (top-boson)
- $|y^Z|$
- $\cos\theta_Z^*$
- p_T^t (four-quark)
- $|\Delta\phi(t\bar{t}, Z)|$
- $|y^{t\bar{t}Z}|$

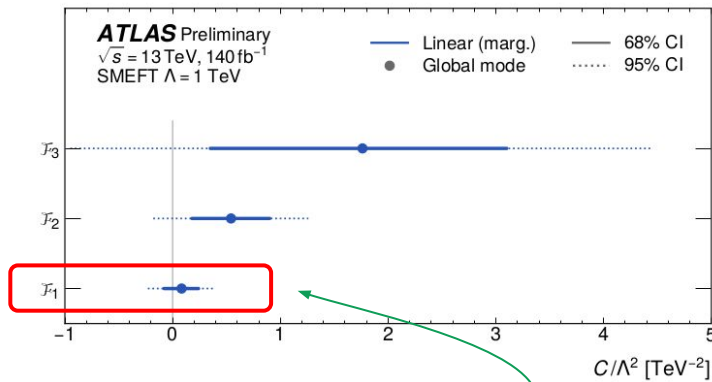
SMEFT results

- **No significant deviations** from the SM prediction
- **Quadratic terms particularly important for four-quark operators**
- For some operators (C_{tG} , C_{tW} , ...) linear terms missing due to vanishing interference at LO in QCD
- **Linear combinations** of operators could provide **more stringent limits**
→ Fisher information matrix



Fisher information matrix

- SMEFT interpretation in the **rotated Warsaw basis**
- **3** most prominent directions of sensitivity
- **Fisher information matrix:**
 - **Inverse covariance matrix** from the linear fit rotated into the space of Wilson coefficients
 - Provides **measure of sensitivity** achievable along directions given by the **eigenvectors**
 - Inverse square root of **eigenvalues λ** estimates expected limits for $F_1 - F_3$
- **Final EFT fit** of 3 best linear combinations \rightarrow yields **most stringent limits on F_1** $[-0.08, 0.24]$



λ ATLAS Preliminary $\sqrt{s} = 13 \text{ TeV}, 140 \text{ fb}^{-1}$

#	λ	$\Re[C_{1g}]$	$\Re[C_{1W}]$	$\Re[C_{1B}]$	$C_{HQ}^{(1)}$	$C_{HQ}^{(3)}$	C_{Ht}	$C_{Qd}^{(8)}$	$C_{Qq}^{(1,8)}$	$C_{Qq}^{(3,1)}$	$C_{Qq}^{(3,8)}$	$C_{Qu}^{(8)}$	$C_{td}^{(8)}$	$C_{dt}^{(8)}$	$C_{tu}^{(8)}$
1	40	0.75			0.23	-0.15	-0.13	-0.10	-0.42	-0.15	0.06	-0.13	-0.05	-0.33	-0.08
2	8	-0.41	0.04	-0.02	-0.34	0.27	0.18	-0.12	-0.57	-0.22	-0.05	-0.22	-0.05	-0.39	-0.12
3	0.5	-0.07	0.06		0.18	0.04	-0.33	-0.07	0.13	0.04	-0.68	-0.42	-0.11	0.08	-0.41

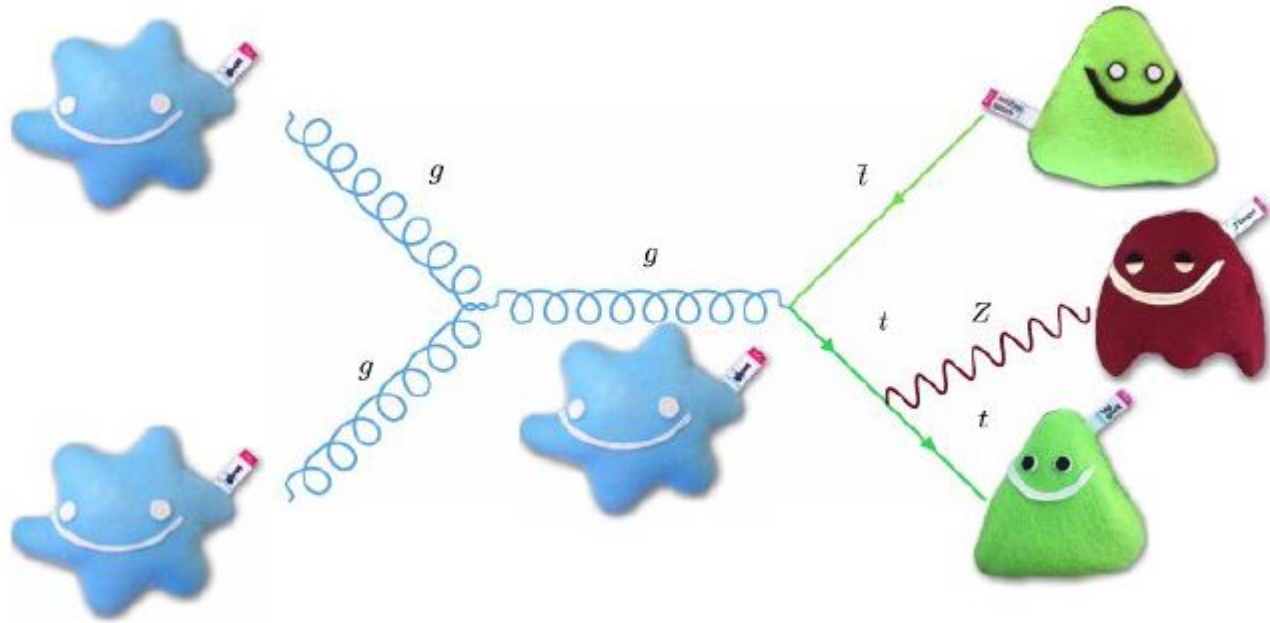
Color scale: 1 (blue), 0 (white), -1 (yellow)

Dominates because of large impact on $gg \rightarrow t\bar{t}$

Summary

- **Legacy $t\bar{t}Z$ measurement** with full Run 2 data
- **Improves previous ATLAS results** re-using the same data but with novel techniques
- **Very precise inclusive x_s measurement (6.5% precision)** → even more than NLO theory (10%)
 - Good compatibility with the theory prediction
- **Differential measurements improved significantly** by using PLU instead of IBU (30% reduction of uncertainties)
 - In agreement with the SM, but still **statistically limited**
- **First spin correlation interpretation** for the $t\bar{t}Z$ process (analysis **statistically limited**)
 - Result consistent with the SM value, **spin-off hypothesis rejected with 1.8σ**
- **Thorough SMEFT interpretation** (20 operators), including **Fisher information matrix** to identify sensitive directions in the coefficient space

Analysis strategy adapted for future combinations!



Thank you for your attention!

BACKUP

MC Samples

Process	Generator	Parton Shower	PDF	Reference Cross Section (fb)
$t\bar{t}Z$	MADGRAPH5_AMC@NLO 2.8.1	PYTHIA 8.244	NNPDF3.0NLO	876.4 [19, 54]
$t\bar{t}H$	MADGRAPH5_AMC@NLO 2.6.0	PYTHIA 8.230	NNPDF3.0NLO	507.4 [19]
$t\bar{t}W/t\bar{t}Wj$	SHERPA 2.2.10	SHERPA 2.2.10	NNPDF3.0NNLO	722.4 [68]
tZq	MADGRAPH5_AMC@NLO 2.9.5	PYTHIA 8.245	NNPDF3.0NLO	38.72
tWZ	MADGRAPH5_AMC@NLO 2.2.2	PYTHIA 8.212	NNPDF2.3LO	16.08
$t\bar{t}$	POWHEG Box 2	PYTHIA 8.230	NNPDF3.0NLO	87,710 [69]
$WZ+\text{jet}/ZZ+\text{jets}$	SHERPA 2.2.2	SHERPA 2.2.2	NNPDF3.0NNLO	7,334
$V+\text{jets}$	SHERPA 2.2.1	SHERPA 2.2.1	NNPDF3.0NNLO	$6,255 \times 10^3$ [67]
$t\bar{t}t\bar{t}$	MADGRAPH5_AMC@NLO 2.3.3	PYTHIA 8.230	NNPDF3.1NLO	11.97 [70]
$t\bar{t}t$	MADGRAPH 2.2.2	PYTHIA 8.186	NNPDF2.3LO	1.64
VH	PYTHIA 8.186	PYTHIA 8.186	NNPDF2.3LO	2,250 [71–77]
VVV	SHERPA 2.2.2	SHERPA 2.2.2	NNPDF3.0NLO	13.74

Region Definitions

Trilepton

Variable	Preselection		
N_ℓ ($\ell = e, \mu$)	= 3		
	≥ 1 OSSF lepton pair with $ m_{\ell\ell} - m_Z < 10$ GeV for all OSSF combinations: $m_{\text{OSSF}} > 10$ GeV		
p_T (ℓ_1, ℓ_2, ℓ_3)	> 27, 20, 15 GeV		
N_{jets} ($p_T > 25$ GeV)	≥ 3		
$N_{b\text{-tagged jets}}$	≥ 1@85%		
	SR-3ℓ-ttZ	SR-3ℓ-tZq	SR-3ℓ-WZ
DNN-tZq output	< 0.40	≥ 0.40	—
DNN-WZ output	< 0.22	< 0.22	≥ 0.22
$N_{b\text{-tagged jets}}$	—	—	≥ 1@60%

Dilepton

Variable	Preselection		
N_ℓ ($\ell = e, \mu$)	= 2		
	= 1 OSSF lepton pair with $ m_{\ell\ell} - m_Z < 10$ GeV		
p_T (ℓ_1, ℓ_2)	> 30, 15 GeV		
	SR-2ℓ-5j2b	SR-2ℓ-6j1b	SR-2ℓ-6j2b
N_{jets} ($p_T > 25$ GeV)	= 5	≥ 6	≥ 6
$N_{b\text{-tagged jets@77\%}}$	≥ 2	= 1	≥ 2

Tetralepton

Variable	Preselection	
N_ℓ ($\ell = e, \mu$)	= 4	
	≥ 1 OSSF lepton pair with $ m_{\ell\ell} - m_Z < 20$ GeV for all OSSF combinations: $m_{\text{OSSF}} > 10$ GeV	
p_T ($\ell_1, \ell_2, \ell_3, \ell_4$)	> 27, 7, 7, 7 GeV	
The sum of lepton charges	= 0	
N_{jets} ($p_T > 25$ GeV)	≥ 2	
$N_{b\text{-tagged jets}}$	≥ 1@85%	
	SR-4ℓ-SF	SR-4ℓ-DF
$\ell\ell^{\text{non-Z}}$	e^+e^- or $\mu^+\mu^-$	$e^\pm\mu^\mp$
DNN output	≥ 0.4	—

Particle & parton-level selection

Particle - after ttZ decay, including hadronisation

- simulates detector level selection

Parton - before ttZ decay, after QCD radiation

- tau leptons excluded

Leptons dressed with additional photons at particle level, but not parton

Particle-level selection	
3 ℓ channel	4 ℓ channel
Exactly 3 leptons, with $p_T(\ell_1, \ell_2, \ell_3) > 27, 20, 15$ GeV	Exactly four leptons, with $p_T(\ell_1, \ell_2, \ell_3, \ell_4) > 27, 7, 7, 7$ GeV
The sum of charges is ± 1	The sum of charges is $= 0$
At least 3 jets, with $p_T > 25$ GeV	At least 2 jets, with $p_T > 25$ GeV
At least 1 b -jet (jet ghost-matched to a b -hadron)	
At least one OSSF lepton pair, with $ m_{\ell\ell} - m_Z < 10$ GeV	
Parton-level selection	
3 ℓ channel	4 ℓ channel
$t\bar{t} \rightarrow e^\pm/\mu^\pm + \text{jets}$	$t\bar{t} \rightarrow e^\pm\mu^\mp/e^\pm e^\mp/\mu^\pm\mu^\mp$
$Z \rightarrow e^\pm e^\mp/\mu^\pm\mu^\mp$	
$ m_{\ell\ell} - m_Z < 15$ GeV	

Top quark reconstruction

- **2I**
 - **Multihypothesis t/W reconstruction**
 - targets fully hadronic tt system; several hypotheses for the number of missing and present top quarks and W bosons
 - 5 different scenarios (1t1W, 2t, 2W, 1t, 1W) tested for each jets-quarks assignment, one with the highest output weight considered correct
 - output weights used as discriminating variables for DNNs
 - **SPANet**
 - symmetry preserving attention neural network, originally developed for the all-hadronic tt events
 - redesigned for the ttZ topology, inputs are jet kinematic and b-tagging info + correct jet assignments
 - trained on the 6j1b events, used to construct discriminating variables for separation DNNs
- **3I**
 - first reconstructed **leptonic-side top**
 - neutrino momentum in z direction from the quadratic equation, most likely top candidate from comparison with $m_{b\nu}$ distribution
 - second b used for the reconstruction of **hadronic top**, two light jets from interpolation of m_{jj}
- **4I**
 - full tt reconstruction using **Two Neutrino Scanning Method**
 - whole eta-phi space scanned for the two neutrinos + 2 leptons not associated with the Z + 2 jets with the highest b-tagging score
 - kinematic constraints from reference distributions used to create output weight - largest taken as correct + weight used as a discriminating variable in DNNs

2l NN variables

Variable	Definition
H_T	sum of p_T of all objects (jets and leptons) in the event
H_T^{jets}	sum of p_T of all jets in the event
$p_T^{X,\text{jet}}$	p_T of the Xth jet, where only the first 8 jets are considered
$p_T^{X,\text{lep}}$	p_T of the Xth lepton
W_{1l1W}	weight for one-top hypothesis and 1W from multihypothesis hadronic t/W reconstruction. It is the probability that the event contains all 3 jets from one of the top quark and two light jets from the decay of the other top quark. More details are provided in Section 5.5.
W_{1t}	weight for one-top hypothesis from multihypothesis hadronic t/W reconstruction. The same as W_{1l1W} , with one top quark only.
$Centr_{\text{jets}}$	scalar sum of p_T divided by sum of E for all jets
$\Delta R(b_1, b_2)$	ΔR between two jets with highest b -tagging working point. The jets with the same working point are ordered by p_T .
H_1^{jets}	first Fox-Wolfram moment built from jets only. The first Fox-Wolfram moment is defined as $H_1 = \sum_{i,j} \frac{\vec{p}_i \cdot \vec{p}_j}{E_{vis}^2}$, where \vec{p}_i and \vec{p}_j are 3-momenta of i-th and j-th object (jet or lepton) and E_{vis} is all visible energy in the event.
$N_{jj}^{m < 50\text{GeV}}$	number of jj combinations with mass lower than 50 GeV
m_Z, y^Z, p_T^Z	mass, rapidity and transverse momentum of Z boson
$minM_{jj}^{\text{ave}}$	average (over the number of jets in event) minimum invariant mass of jet pairs. For each jet, the other jet which results in the minimum dijet invariant mass is found. The observable is the average of these masses over all jets in the event.
$\Delta R(l, l)$	ΔR between two leptons
$PCBT_{Xj}$	discretised b -tagging efficiency (100-85-77-70-60%) of the Xth jet
$N_{\text{lep}}^{\text{top}}$	number of leptonic top candidates
$N_{\text{had}}^{\text{top}}$	number of hadronic top candidates
N_{had}^W	number of hadronic W candidates
E_T^{miss}	missing transverse energy in the event
H_1	first Fox-Wolfram moment built from jets and leptons
$p_T^{\tilde{t}\tilde{t}, \text{spanet}}$	transverse momentum of the $\tilde{t}\tilde{t}$ system reconstructed from jets predicted by SPANet

31 NN variables

Variable	Definition
PCBT _{b1}	highest discretised b -tagging efficiency (100-85-77-70-60%) of all jets in the event.
PCBT _{b2}	second highest discretised b -tagging efficiency of all jets in the event.
Jet $p_{T,i}$	transverse momentum of the i 'th jet in the event where $i \in [1, 4]$
E_T^{miss}	missing transverse energy of the event
Lepton $p_{T,i}$	transverse momentum of the i 'th lepton in the event where $i \in [1, 3]$
m_t^{lep}	reconstructed mass of the leptonically decaying top quark
m_t^{had}	reconstructed mass of the hadronically decaying top quark
N_{jets}	jet multiplicity in event
Leading b -tagged jet p_T	transverse momentum of the jet with the highest discretised b -tagging efficiency. If two have the same bin the leading p_T jet of the two is used.
H_T	sum of the transverse momentum of all jets in the event
$\Delta R(l_i, b_1)$	distance in ΔR between the i 'th lepton and the b -tagged jet tagged with the highest working point in the event where $i \in [1, 3]$
$p_{T,i}^Z$	transverse momentum of the first and second lepton ($i \in [1, 2]$) assigned to the Z boson based on their invariant mass being closest to the Z mass
η_i^Z	pseudo-rapidity of the first and second lepton ($i \in [1, 2]$) assigned to the Z boson based on their invariant mass being closest to the Z mass
Lepton $p_T^{\text{non-Z}}$	transverse momentum of the remaining lepton not assigned to the Z boson

41 NN variables

Variable	Definition	SF	DF
E_T^{miss}	the missing transverse energy in the event	✓	—
$m^{\ell\ell, non-Z}$	the invariant mass of two leptons which were not reconstructed as originating from Z	✓	✓
2 ν SM weight	the output of the <i>Two neutrino scanning method</i> for event	✓	✓
p_T^Z	the transverse momentum of OSSF lepton pair identified as Z pair (invariant mass of lepton pair closest to Z mass)	✓	✓
$m_i^{\ell b}$	the invariant mass of lepton and b -tagged jet reconstructed as originating from top by <i>Two neutrino scanning method</i>	✓	✓
$m_{\bar{i}}^{\ell b}$	the invariant mass of lepton and b -tagged jet reconstructed as originating from antitop by <i>Two neutrino scanning method</i>	✓	✓
PCBT $_{b1}$	highest discretised b -tagging efficiency (100-85-77-70-60%) of all jets in the event.	✓	—
$p_T^{\text{lep}_1}$	the transverse momentum of the leading lepton	✓	✓
$p_T^{\text{jet}_2}$	the transverse momentum of the sub-leading jet	✓	✓
PCBT $_{b2}$	second highest discretised b -tagging efficiency of all jets in the event.		
N_{jets}	jet multiplicity in event	—	✓
$N_{b\text{-tagged jets}}$	b -tagged jet multiplicity in event	—	✓

Backgrounds

Dilepton tt regions

Variable	Preselection		
N_ℓ ($\ell = e, \mu$)	= 2 = 1 OSDF lepton pair with $ m_{\ell\ell} - m_Z < 10$ GeV		
$p_T(\ell_1, \ell_2)$	> 30, 15 GeV		
	2ℓ-eμ-5j2b	2ℓ-eμ-6j1b	2ℓ-eμ-6j2b
N_{jets} ($p_T > 25$ GeV)	= 5	≥ 6	≥ 6
$N_{b\text{-tagged jets@77\%}}$	≥ 2	= 1	≥ 2

Tetralepton ZZ CR

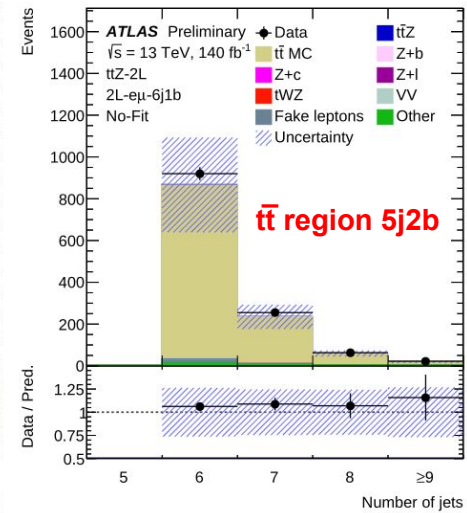
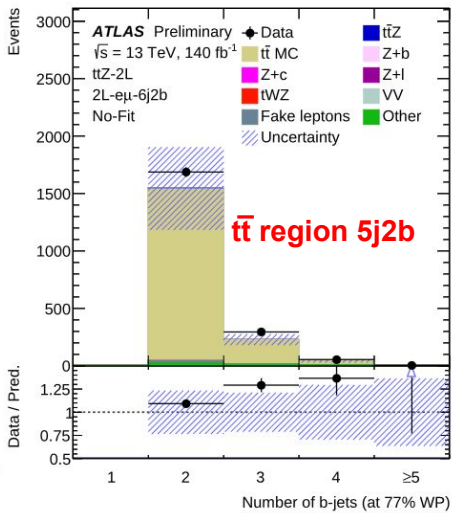
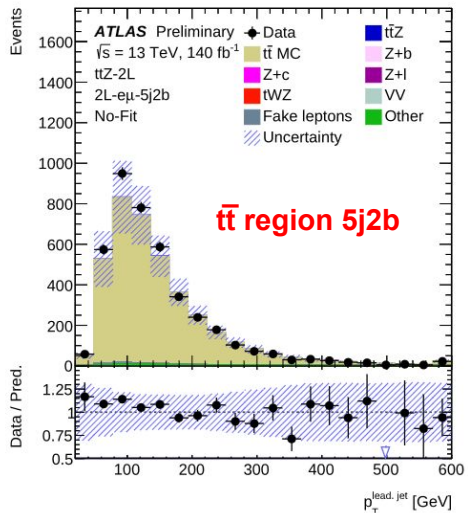
Variable	Preselection
N_ℓ ($\ell = e, \mu$)	= 4 ≥ 1 OSSF lepton pair with $ m_{\ell\ell} - m_Z < 20$ GeV for all OSSF combinations: $m_{\text{OSSF}} > 10$ GeV
$p_T(\ell_1, \ell_2, \ell_3, \ell_4)$	> 27, 7, 7, 7 GeV
The sum of lepton charges	= 0
N_{jets} ($p_T > 25$ GeV)	≥ 2
$N_{b\text{-tagged jets}}$	≥ 1 @85%
	CR-4ℓ-ZZ
$\ell\ell^{\text{non-Z}}$	e^+e^- or $\mu^+\mu^-$
DNN-SF output	< 0.4

Fake CRs in 3l and 4l

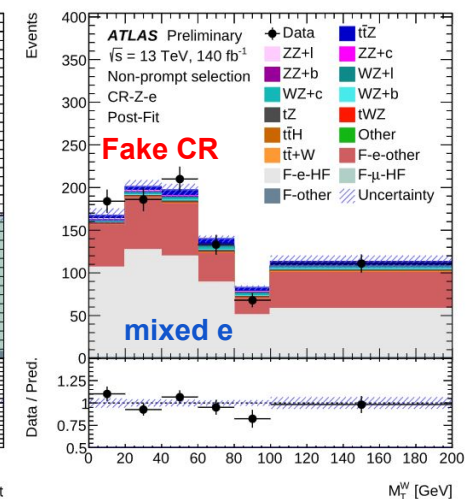
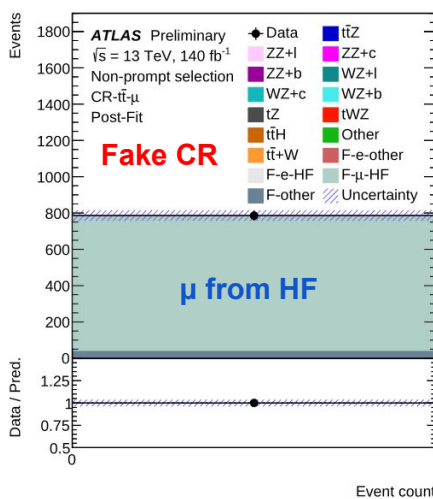
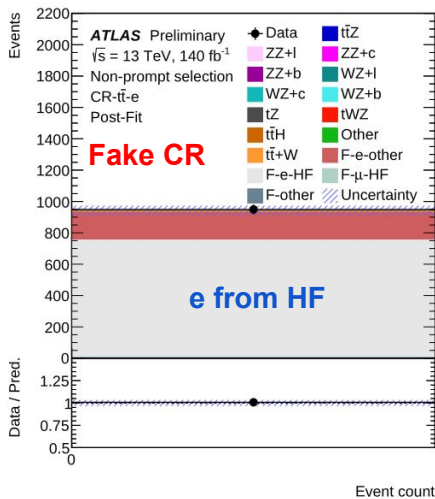
Variable	Preselection		
N_ℓ ($\ell = e, \mu$)	= 3 (of which = 1 loose non-tight)		
$p_T(\ell_1, \ell_2, \ell_3)$	> 27, 20, 15 GeV		
Sum of lepton charges	± 1		
N_{jets} ($p_T > 25$ GeV)	≥ 3		
$N_{b\text{-tagged jets}}$	≥ 1 @85%		
	CR-t\bar{t}-e	CR-t\bar{t}-μ	CR-Z-e
Lepton flavours	no OSSF pair (loose lepton is an electron)	no OSSF pair (loose lepton is a muon)	OSSF pair (exactly 3 electrons)
E_T^{miss}	—	—	< 80 GeV

Backgrounds

- $t\bar{t}$ regions in 2l channel



- Fake CRs in 3l and 4l channels



Systematics

Theory

Signal:

- **Nominal $t\bar{t}Z$:** aMC@NLO + Pythia 8
- **Parton shower:** Pythia 8 vs. Herwig 7
- **Scales:** μ_R, μ_F varied up and down by a factor of 2
- **ISR:** varying Var3c parameter of Pythia A14 tune
- **PDF:** PDF4LHC prescription
- modelling cross-checked with Sherpa 2.2.1

Background:

- **WZ/ZZ + jets:** CKKW, QSF, μ_R, μ_F , PDFs, normalisations 10-30%
- **tZq:** parton shower (P8 vs. H7), PDFs, ISR and μ_R, μ_F
- **tWZ:** DR1 vs. DR2 diagram removal scheme, PDFs, μ_R, μ_F
- **Z+jets:** CKKW, QSF, PDFs, μ_R, μ_F , 10% normalisation for Z+l

Experimental

- **Luminosity** (0.83%)
- **Pileup** reweighting
- **Lepton selection** (1-3%)
- **Jet selection:** JER, JES, JVT
- **Flavor tagging** (1.7%)
- E_T^{miss}

Experimental uncertainties allow for the future combinations !

2l post-fit yields and norm. factors

	SR-2 l -5j2b	SR-2 l -6j2b	SR-2 l -6j1b
$t\bar{t}Z$	297 \pm 20	443 \pm 27	305 \pm 28
$t\bar{t}DD$	4001 \pm 72	1913 \pm 45	1161 \pm 35
$Z+b$	5710 \pm 170	2680 \pm 110	4830 \pm 280
$Z+c$	349 \pm 95	189 \pm 47	2020 \pm 480
$Z+l$	59 \pm 25	19.6 \pm 8.1	1020 \pm 240
tWZ	23.2 \pm 0.92	34.4 \pm 2.1	40.2 \pm 1.9
Diboson	150 \pm 80	95 \pm 52	340 \pm 180
Fake leptons	28 \pm 14	18.6 \pm 9.2	25 \pm 12
Other	55 \pm 25	49 \pm 22	23 \pm 10
Total	10700 \pm 100	5440 \pm 68	9760 \pm 110
Data	10702	5435	9737

Norm. factor	Value
\mathcal{N}_{ZZ+b}	1.1 $^{+0.4}_{-0.4}$
\mathcal{N}_{WZ+b}	0.9 $^{+0.4}_{-0.4}$
\mathcal{N}_{Z+b}	1.08 $^{+0.11}_{-0.10}$
\mathcal{N}_{Z+c}	0.61 $^{+0.23}_{-0.20}$
$\mathcal{N}_{e,\text{HF}}$	0.89 $^{+0.09}_{-0.09}$
$\mathcal{N}_{e,\text{other}}$	1.2 $^{+0.4}_{-0.4}$
$\mathcal{N}_{\mu,\text{HF}}$	1.02 $^{+0.08}_{-0.08}$

3l & 4l post-fit yields

	SR-3 ℓ -ttZ	SR-3 ℓ -WZ	SR-3 ℓ -tZq	SR-4 ℓ -SF	SR-4 ℓ -DF	CR-4 ℓ -ZZ
$t\bar{t}Z$	441 \pm 21	49.0 \pm 3.7	151 \pm 11	49.4 \pm 3.0	51.1 \pm 2.9	2.36 \pm 0.23
$t\bar{t}W$	4.3 \pm 2.2	2.2 \pm 1.1	5.3 \pm 2.6	—	—	—
$t\bar{t}H$	11.9 \pm 1.1	1.43 \pm 0.13	6.70 \pm 0.57	2.79 \pm 0.24	2.82 \pm 0.24	0.32 \pm 0.04
WZ + b	21.1 \pm 7.4	47 \pm 16	27.1 \pm 9.5	—	—	—
WZ + c	8.9 \pm 3.6	12.2 \pm 5.0	11.1 \pm 4.6	—	—	—
WZ + l	1.19 \pm 0.52	1.70 \pm 0.76	1.81 \pm 0.80	—	—	—
ZZ + b	4.3 \pm 2.5	6.9 \pm 4.0	7.3 \pm 4.2	7.5 \pm 2.0	0.46 \pm 0.12	26.7 \pm 6.9
ZZ + c	1.23 \pm 0.42	1.22 \pm 0.43	1.61 \pm 0.53	2.13 \pm 0.66	0.30 \pm 0.09	24.6 \pm 7.1
ZZ + l	0.42 \pm 0.13	0.26 \pm 0.09	0.53 \pm 0.15	0.83 \pm 0.24	0.34 \pm 0.09	22.6 \pm 5.2
tZq	20.8 \pm 4.0	13.2 \pm 2.3	99 \pm 16	—	—	—
tWZ	40.0 \pm 7.6	18.0 \pm 4.2	24.2 \pm 3.0	6.60 \pm 0.82	7.3 \pm 1.2	0.69 \pm 0.10
$t\bar{t}t\bar{t}$	1.56 \pm 0.78	0.13 \pm 0.07	0.27 \pm 0.14	—	—	—
Other	1.33 \pm 0.61	1.40 \pm 0.63	0.39 \pm 0.19	0.55 \pm 0.25	1.12 \pm 0.52	0.55 \pm 0.25
F-e-HF	4.6 \pm 1.0	3.90 \pm 0.87	12.0 \pm 2.6	0.28 \pm 0.07	0.45 \pm 0.10	0.11 \pm 0.03
F-e-Other	7.8 \pm 2.7	7.3 \pm 2.6	15.2 \pm 5.4	0.39 \pm 0.14	0.50 \pm 0.18	0.10 \pm 0.04
F-m-HF	6.98 \pm 0.86	5.27 \pm 0.66	18.2 \pm 2.2	0.58 \pm 0.07	0.62 \pm 0.08	0.16 \pm 0.02
F-Other	2.8 \pm 1.2	2.7 \pm 1.2	4.4 \pm 2.0	0.90 \pm 0.40	1.66 \pm 0.74	0.33 \pm 0.15
Total	580 \pm 19	174 \pm 13	386 \pm 15	72.0 \pm 3.4	66.7 \pm 3.0	78.5 \pm 8.0
Data	569	175	388	79	74	81

Profile likelihood unfolding procedure

The profile likelihood unfolding procedure uses the following formula for the likelihood

$$L(\vec{n}|\mu, \vec{\theta}, \vec{k}) = \prod_{r \in \text{regions}} \prod_{i \in \text{bins}} \text{Pois}(n_{i,r} | \vec{\mu} \vec{S}_{i,r}(\vec{\theta}) + B_{i,r}(\vec{\theta}, \vec{k})) \times \prod_{j \in \text{NPs}} \text{Gaus}(\theta_j) \times R(\vec{\mu}), \quad (2)$$

where $n_{i,r}$ is the number of events observed in i -th bin of r -th region, $\vec{S}_{i,r}$ is the response matrix, $B_{i,r}(\vec{\theta}, \vec{k})$ is the background contribution, \vec{k} is vector of free-floating background normalisations and $\vec{\theta}$ is vector of nuisance parameters related to the systematic uncertainties. In case of the normalised distribution, the $\vec{\mu}$ is reparametrised in the way, that the last element of the vector is the overall signal normalisation. In this case, the content of the last bin of the unfolded distribution is dropped from the $\vec{\mu}$, since it is no longer a free parameter and it can be calculated based on the values in other bins and the overall normalisation.

$$\rho = \left\langle \sqrt{1 - (C_{ii} C_{ii}^{-1})^{-1}} \right\rangle, \quad (4)$$

where C_{ii} is the correlation matrix, C_{ii}^{-1} is inverted correlation matrix and the brackets represent the mean value over the diagonal elements. The τ value where the global correlation reaches its minimum was chosen as the optimal value.

Differential observables

Observable	Channels	Bins	Bin Ranges
p_T^Z [GeV]	$3\ell + 4\ell$	8	[0, 60, 100, 140, 180, 230, 280, 350, 1000]
$ y^Z $	$3\ell + 4\ell$	9	[0, 0.125, 0.275, 0.425, 0.6, 0.775, 0.95, 1.175, 1.45, 2.5]
$p_T^{\ell, \text{non-Z}}$	3ℓ	5	[0, 35, 55, 80, 120, 500]
$ \Delta y(Z, t_{\text{lep}}) $	3ℓ	5	[0, 0.25, 0.6, 1.05, 1.55, 5]
$ \Delta\phi(Z, t_{\text{lep}}) $	3ℓ	6	[0, 0.16, 0.44, 0.66, 0.82, 0.93, 1]
$ \Delta\phi(\ell_t^+, \ell_{\bar{t}}^-) $	4ℓ	7	[0, 0.2, 0.37, 0.53, 0.67, 0.79, 0.89, 1]
H_T^ℓ	3ℓ	8	[50, 130, 165, 195, 230, 275, 330, 405, 800]
H_T^ℓ	4ℓ	5	[50, 195, 250, 315, 400, 800]
N_{jets}	3ℓ	4	[2.5, 3.5, 4.5, 5.5, 10.5]
N_{jets}	4ℓ	3	[1.5, 2.5, 3.5, 8.5]
p_T^t [GeV]	$3\ell + 4\ell$	10	[0, 48, 80, 112, 144, 176, 216, 256, 296, 352, 800]
$p_T^{t\bar{t}}$ [GeV]	$3\ell + 4\ell$	10	[0, 50, 80, 110, 140, 170, 210, 250, 290, 330, 1000]
$ \Delta\phi(t\bar{t}, Z) /\pi$	$3\ell + 4\ell$	5	[0, 0.73, 0.86, 0.94, 0.98, 1]
$m_{t\bar{t}}$ [GeV]	$3\ell + 4\ell$	10	[0, 370, 420, 470, 530, 600, 680, 780, 890, 1010, 2000]
$m_{t\bar{t}Z}$ [GeV]	$3\ell + 4\ell$	10	[400, 580, 650, 720, 800, 890, 990, 1100, 1220, 1350, 2000]
$ y^{t\bar{t}Z} $	$3\ell + 4\ell$	10	[0, 0.075, 0.2, 0.35, 0.5, 0.65, 0.8, 0.95, 1.1, 1.25, 2.5]
$\cos\theta_Z^*$	$3\ell + 4\ell$	8	[-1, -0.75, -0.5, -0.25, 0, 0.25, 0.5, 0.75, 1]

Spin correlations

- **k, n, r** - axes in orthonormal basis, +/- is charge of lepton/quark
- In **4l** observables defined using **leptons from $t\bar{t}$**
- In **3l** necessary to use **lepton + down-type quark** from W decay (c or s) - c tagged jets if pass at least 85% but fail 60% (its companion is s-quark)
- **Negative (or >1) f_{SM}** caused by large variability of the fit results under local excesses not compatible with either the spin-on or spin-off templates
- **Fit enhances the impact of systematic uncertainties with an important shape component** (alternative parton showers for $t\bar{t}Z$, electron isolation and $ZZ+b$ scale uncertainties in 4l)
- **Future spin density measurements** will be able to probe possible **CP-violation effects** and **4-fermion operators**

A final observable of interest can be constructed in both the 3ℓ and 4ℓ channels: the opening angle between the two charged leptons (charged lepton and s -jet) from the dileptonic (semi-leptonic) $t\bar{t}$ system, where each decay product is first boosted to the rest frame of its respective parent (anti-)top quark. This angle φ is particularly sensitive to spin correlations, and the following three relations hold [26]:

$$\frac{1}{\sigma} \frac{d\sigma}{d\cos\varphi} = \frac{1}{2} (1 - D \cos\varphi), \quad D = -\frac{c_{rr} + c_{kk} + c_{nn}}{3}, \quad D = -3\langle\cos\varphi\rangle. \quad (6)$$

SMEFT interpretation

$$\mathcal{L}_{\text{SMEFT}} = \mathcal{L}_{\text{SM}} + \sum_{d>4} \mathcal{L}^{(d)}, \quad \mathcal{L}^{(d)} = \sum_{i=1}^{n_d} \frac{C_i^{(d)}}{\Lambda^{d-4}} Q_i^{(d)},$$

$$c_{tZ} = -\sin\theta_W C_{tB} + \cos\theta_W C_{tW},$$

$$c_{\varphi Q}^- = C_{HQ}^{(1)} - C_{HQ}^{(3)},$$

Wilson coefficient	68% CI (exp.)	95% CI (exp.)	68% CI (obs.)	95% CI (obs.)	Best-fit
\mathcal{F}_1 $\mathcal{O}(\Lambda^{-2})$ (marg.)	[-0.15, 0.16]	[-0.30, 0.31]	[-0.080, 0.24]	[-0.23, 0.39]	0.08
\mathcal{F}_2 $\mathcal{O}(\Lambda^{-2})$ (marg.)	[-0.36, 0.36]	[-0.72, 0.70]	[0.18, 0.90]	[-0.18, 1.3]	0.5
\mathcal{F}_3 $\mathcal{O}(\Lambda^{-2})$ (marg.)	[-1.4, 1.3]	[-2.7, 2.7]	[0.35, 3.1]	[-0.95, 4.5]	2

	Operator	Definition	
top-boson	Q_{tW}	$(\bar{Q}\sigma^{\mu\nu}t)\sigma^i\tilde{H}W_{\mu\nu}^i$	(★)
	Q_{tB}	$(\bar{Q}\sigma^{\mu\nu}t)\tilde{H}B_{\mu\nu}$	(★)
	Q_{tG}	$(\bar{Q}\sigma^{\mu\nu}T^a t)\tilde{H}G_{\mu\nu}^a$	(★)
	$Q_{HQ}^{(1)}$	$(H^\dagger i\overleftrightarrow{D}_\mu H)(\bar{Q}\gamma^\mu Q)$	
	$Q_{HQ}^{(3)}$	$(H^\dagger i\overleftrightarrow{D}_\mu^i H)(\bar{Q}\sigma^i\gamma^\mu Q)$	
	Q_{Ht}	$(H^\dagger i\overleftrightarrow{D}_\mu H)(\bar{t}\gamma^\mu t)$	
four-quark	$Q_{tu}^{(1)}$	$(\bar{t}\gamma_\mu t)(\bar{u}\gamma^\mu u)$	
	$Q_{tu}^{(8)}$	$(\bar{t}T^a\gamma_\mu t)(\bar{u}T^a\gamma^\mu u)$	
	$Q_{td}^{(1)}$	$(\bar{t}\gamma_\mu t)(\bar{d}\gamma^\mu d)$	
	$Q_{td}^{(8)}$	$(\bar{t}T^a\gamma_\mu t)(\bar{d}T^a\gamma^\mu d)$	
	$Q_{qt}^{(1)}$	$(\bar{q}\gamma_\mu q)(\bar{t}\gamma^\mu t)$	
	$Q_{qt}^{(8)}$	$(\bar{q}T^a\gamma_\mu q)(\bar{t}T^a\gamma^\mu t)$	
	$Q_{Qu}^{(1)}$	$(\bar{Q}\gamma_\mu Q)(\bar{u}\gamma^\mu u)$	
	$Q_{Qu}^{(8)}$	$(\bar{Q}T^a\gamma_\mu Q)(\bar{u}T^a\gamma^\mu u)$	
	$Q_{Qd}^{(1)}$	$(\bar{Q}\gamma_\mu Q)(\bar{d}\gamma^\mu d)$	
	$Q_{Qd}^{(8)}$	$(\bar{Q}T^a\gamma_\mu Q)(\bar{d}T^a\gamma^\mu d)$	
	$Q_{Qq}^{(1,1)}$	$(\bar{Q}\gamma_\mu Q)(\bar{q}\gamma^\mu q)$	
$Q_{Qq}^{(3,1)}$	$(\bar{Q}\sigma^i\gamma_\mu Q)(\bar{q}\sigma^i\gamma^\mu q)$		
$Q_{Qq}^{(1,8)}$	$(\bar{Q}T^a\gamma_\mu Q)(\bar{q}T^a\gamma^\mu q)$		
$Q_{Qq}^{(3,8)}$	$(\bar{Q}\sigma^i T^a\gamma_\mu Q)(\bar{q}\sigma^i T^a\gamma^\mu q)$		